# Magnetic interactions in a ferromagnetic honeycomb nanoscale network

M. Tanaka,* E. Saitoh, and H. Miyajima

*Department of Physics, Keio University, 3-14-1 Hiyoshi, Yokohama 223-8522, Japan*

T. Yamaoka

*SII NanoTechnology Inc., 563 Takatsuka-Shinden, Matsudo 270-2222, Japan*

Y. Iye

*Institute for Solid State Physics, University of Tokyo, 5-1-5 Kashiwanoha, Kashiwa 277-8581, Japan*

The magnetic structure and magnetization process in a permalloy wire-based honeycomb network have been investigated by means of magnetic-force microscopy (MFM) and magnetoresistance measurement. The MFM measurements show the remanent magnetic structures to be governed by magnetic interaction similar to the ice rule, which provides a direct analogy between the present honeycomb network and an Ising system on a kagomé lattice. The magnetoresistance measurements reveal that this interaction also dominates the magnetization processes in the network. By decreasing the exchange energy at the vertices of the network, the ice-rule type of interaction causes a transition of the magnetization process in the network.

## I. INTRODUCTION

The development of lithography techniques allows us to fabricate well-defined nanometer-size structures. This provides effective ways to explore magnetics because of ideally controlled domains in ferromagnets, and the magnetic properties of nanoscale magnetic structures have been studied extensively.[1–14] To date, however, few studies have focused on the interaction among such nanoscale magnetic structures. Understanding this interaction is important because of its capability for enabling new magnetic device applications, e.g., magnetic logic devices.[8] In this paper, we investigated a simple kind of honeycomb structure which contains orderly arranged vertices connected to three ferromagnetic wires. We show that, in this system, the magnetic interaction among wires at each vertex is governed by the "magnetic-ice rule," similar to the spin frustration in real geometrically frustrated systems.[15] This ice-rule interaction was found to be controllable in terms of external magnetic fields. The magnetic frustration is crucial in a wide range of static and dynamical magnetic properties,[16–18] and the artificial nanosystem described here provides a way for designing magnetic properties.

## II. EXPERIMENTAL

The permalloy ($Ni_{81}Fe_{19}$) honeycomb nanoscale network was fabricated on a thermally oxidized Si substrate by electron-beam lithography. After the desired pattern was drawn on a spin-coated layer of resist (ZEP-520) and developed, permalloy was deposited in a high vacuum ($1 \times 10^{-8}$ Torr) by electron-beam evaporation. The successful liftoff process allowed the resist mask to be removed and the sample remained on the substrate surface. A scanning electronic microscope image of part of the fabricated honeycomb network is shown in Fig. 1. The size of the sample is

as follows: the width of the wire=50 nm, its length =400 nm, and its thickness=20 nm. The network consists of $60 \times 60$ unit cells in the honeycomb structure.

Magnetic domain observations of the sample in remanent states were carried out with magnetic-force microscopy (MFM, SPI4000/SPA300HV, SII NanoTechnology Inc.). A CoPtCr low moment probe was used to minimize the influence of the stray field from the probe. To measure the resistance of the network, two Cu electrodes were deposited at its edges. The resistance was measured by allowing an electric current $\mathbf{I}$ to flow as shown in Fig. 1. The magnetoresistance was measured by applying external magnetic fields in various directions. Hereafter we denote the field by the in-plane component $H_\parallel$ and the out-of-plane component $H_\perp$. The angle between $\mathbf{I}$ and the projection of the field on the film plane is denoted as $\theta$ (see Fig. 1).

## III. REMANENT MAGNETIC STRUCTURE

In Fig. 2(a), we show an MFM image of the honeycomb network in a remanent state. Before the observation, the
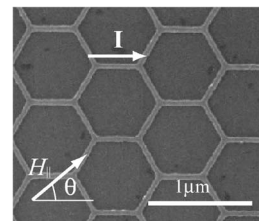


FIG. 1. A scanning electronic microscope image of part of the permalloy wire-based honeycomb structure. The size of the sample is as follows: wire width=50 nm, wire length=400 nm, and thickness=20 nm. The sample consists of $60 \times 60$ unit cells. The arrow $\mathbf{I}$ denotes the direction of the current flow to measure the magnetoresistances.
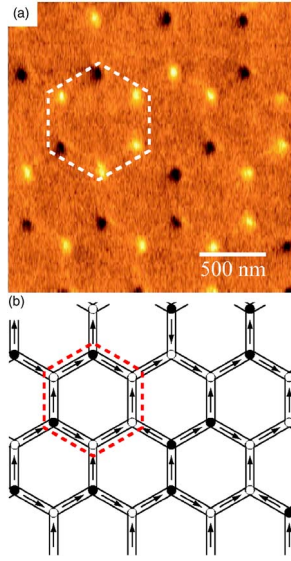
FIG. 2. (Color online) (a) A magnetic-force microscope (MFM) image of the honeycomb nanoscale network in a remanent state. An initial magnetic field (4 kOe) was perpendicular to the network. (b) A schematic illustration of the magnetization configuration corresponding to the MFM image in (a). Open and solid circles on the vertex correspond to the white and black contrasts in the MFM image, respectively. The dashed hexagons in (a) and (b) are merely visual guides representing the same region of the network system.

magnetic field of 4 kOe was applied perpendicular to the network. In this MFM image, bright or dark contrasts at vertices correspond to the stray fields from the magnetic charge on domain walls. No domain wall features were observed in the wire parts. This indicates that each vertex traps the domain wall firmly and that the wire part takes a single domain. The result shows that the magnetic properties of the ferromagnetic network can be described in terms of the uniform magnetization of each wire and their interaction at the vertices.

A schematic magnetic domain configuration corresponding to the MFM image is shown in Fig. 2(b). The open and solid circles on each vertex correspond to the bright and dark contrasts in Fig. 2(a), respectively. Notable is the fact that all the bright contrasts (and all the dark contrasts) are of equal magnitude. This implies that only two types of magnetization configuration actually occur at the vertices of this network, in spite of four possible ones as discussed below. These magnetic configurations minimize the exchange energy at the vertices. The observed configuration of magnetization $\mathbf{M}_i$ in each wire ($i$) was found to be determined such that the vector sum of $\mathbf{M}_i$ for three wires jointed at each vertex $N$, $\Sigma_{i \in N}\mathbf{M}_i$, must not be a zero vector. This is the "two-in/one-out" ($\langle ++- \rangle$) or "one-in/two-out" ($\langle +-- \rangle$) structure around a vertex [see Figs. 3(b) and 3(c)].

The magnetic configuration of the present system can be analyzed as a frustrated system constructed by magnetic moments in the wires. For every vertex, there are six possible magnetic configurations under the ($\langle ++- \rangle$) or ($\langle +-- \rangle$) rule. Such a rule excluding "three-in" ($\langle +++ \rangle$) and "three-out" ($\langle --- \rangle$) magnetic structures [see Figs. 3(a) and 3(d)] is analogous with the so-called ice rule in frustrated systems.[15–18]
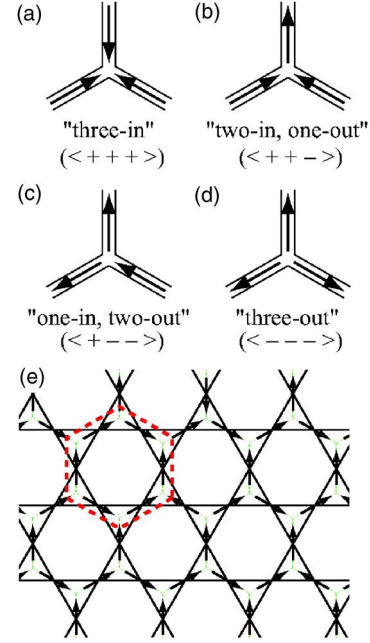


FIG. 3. (Color online) (a)–(d) Possible magnetization configurations at a vertex. (e) A kagomé lattice (solid lines) as Voronoi polygons of the vertices of the honeycomb lattice (dashed lines). Arrows represent magnetic moments. The dashed hexagon in (e) corresponds to the white or dashed hexagons in Figs. 2(a) and 2(b).

The above observation allows the magnetic properties in the present system to be modeled in terms of the following effective energy formula:

$$E(\{\mathbf{M}_i\}) = -J\sum_N \left| \sum_{i \in N} \mathbf{M}_i \right|^2 - \sum_i \mathbf{H} \cdot \mathbf{M}_i, \qquad (1)$$

where $\mathbf{H}$ and $4J|\mathbf{M}_i|^2$ are the external magnetic field and the energy difference between $\Sigma_{i \in N}\mathbf{M}_i \neq 0$ configuration and $\Sigma_{i \in N}\mathbf{M}_i = 0$ configuration, respectively. $\mathbf{M}_i$ is restricted to direct parallel or antiparallel to each of the wire axes. The first term in Eq. (1) is the total magnetic interaction with coupling constant $J$ among the three magnetization vectors at the vertex $N$, while the second term is the total Zeeman energy. Expanding Eq. (1) gives the following simple formula comprising nearest-neighbor interaction and Zeeman term:

$$E(\{\mathbf{M}_i\}) = -2J\sum_{\langle i,j \rangle} \mathbf{M}_i \cdot \mathbf{M}_j - \sum_i \mathbf{H} \cdot \mathbf{M}_i + \text{const}, \qquad (2)$$

where $\Sigma_{\langle i,j \rangle}$ denotes the sum all over the nearest-neighbor pairs of wire parts [see Fig. 3(e)]. This formula shows an analogy between the present wire-based network and the Heisenberg-spin model with a kagomé lattice [see Fig. 3(e)] on strong uniaxial magnetic anisotropy.[16]

## IV. IN-PLANE MAGNETORESISTANCE

The ice rule observed in the remanent magnetic structure also dominates the magnetization process. The curves shown in Fig. 4 exemplify the field dependent magnetoresistance for various field directions $\theta$. At $\theta = 0°$, the wires in the lattice are classified into three groups. They have different angles $\theta_d$
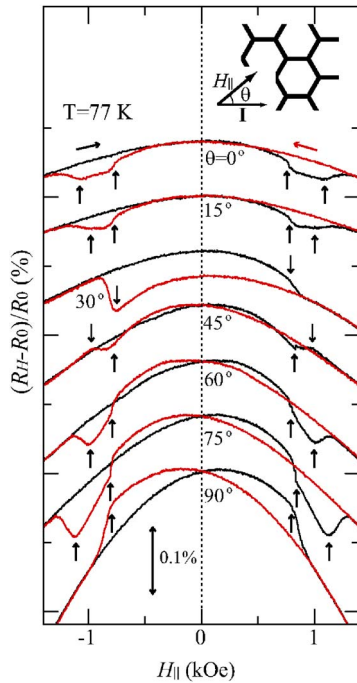
FIG. 4. (Color online) In-plane magnetoresistance curves of the permalloy honeycomb nanoscale network at 77 K. $\theta$ denotes the angle between the magnetic field $H_{\parallel}$ and the current **I**. $R_H$ is the resistance between the Cu electrodes, which were placed at the edges of the sample. $R_0$ is the resistance of the system in the absence of magnetic fields.



FIG. 5. (Color online) Magnetoresistances of the honeycomb nanoscale network at $\theta = 75°$ measured by applying a perpendicular magnetic field $H_{\perp}$. (a) $H_{\parallel}$ dependence of the resistance at $H_{\perp} = 3.5$ kOe. Arrows indicate jumps in magnetoresistance corresponding to magnetization reversals. (b) $H_{\parallel}$ dependence of the resistance at $H_{\perp} = 4.0$ kOe. Arrows indicate jumps in magnetoresistance corresponding to magnetization reversals. (c) $H_{\perp}$ dependence of $H_{SW}$.

with respect to the external magnetic field, i.e., $\theta_d = 0°$, 60°, and −60°. After applying magnetic field of −1.4 kOe, the resistance increases monotonically with increasing fields and it takes a maximum around $H_{\parallel} = 0$. This is due to the anisotropic magnetoresistance (AMR) effect reflecting the deviation of wire magnetization from the wire axis in each wire. By further increasing the field, the resistance shows an abrupt change at 0.8 kOe, corresponding to magnetization reversal in the wires in the two groups of three ones. The following resistance jump at $H_{\parallel} = 1.1$ kOe is due to the reversals of the magnetization in the wires in the other group. Importantly, the number of abrupt changes in resistance is equal to that of the magnetization reversal process and observed to be no more than two for all the $\theta$ values. At $\theta = 75°$, for instance, there are two distinct jumps at $H_{\parallel} = -0.81$ kOe and $H_{\parallel} = -1.1$ kOe. This indicates that there are two distinct magnetization reversals when $\theta = 75°$. Note that, at $\theta = 75°$, three nonequivalent magnetization flips are expected in the absence of the vertex interaction, since each of three groups of wires distinguished by the angles $\theta_d$ reverses at the different in-plane magnetic field. This discrepancy can be interpreted by the magnetic-ice rule prohibiting the $\langle +++ \rangle$ and $\langle --- \rangle$ configurations; according to the ice rule, the number of magnetizing steps is reduced from three to two. In other words, magnetoresistance at $\theta = 75°$ can be used as a probe for detecting magnetic-ice rule in the present system and allows us to further explore the magnetic interaction at the vertices.
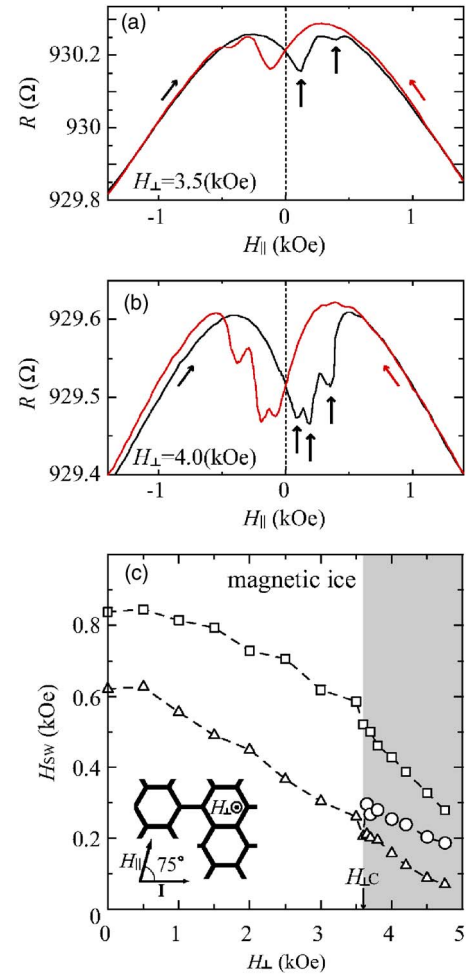
## V. CONTROL OF MAGNETIC-ICE RULE BY EXTERNAL FIELD

So far, we have demonstrated that both the remanent magnetic structure and the magnetization process in the present network are governed by the magnetic-ice rule at the vertices. This implies that the magnetic properties of this system could change by controlling the ice-rule. Here, we demonstrate that the magnetic ice-rule is controllable by an application of magnetic fields.

Figures 5(a) and 5(b) show the magnetoresistance at 90 K as a function of $H_{\parallel}$ at $\theta = 75°$ in a magnetic field, with $H_{\perp}$ applied perpendicular to the film plane. This perpendicular magnetic field $H_{\perp}$ reduces the in-plane component of the magnetization and thus reduces the magnitude of the magnetic interaction in the vertices. As shown in Fig. 5(a), the magnetoresistance curve for $H_{\perp} = 3.5$ kOe shows *two* distinct jumps, which indicate that the magnetic-ice rule governs the magnetization process for $H_{\perp} = 3.5$ kOe. In contrast, as

shown in Fig. 5(b), magnetoresistance at $H_\perp = 4.0$ kOe exhibits *three* clear discontinuities, which indicates that there are three nonequivalent magnetization reversals. This shows that $\langle +++\rangle$ or $\langle ---\rangle$ magnetic structures, which are inhibited between $H_\perp = 0$ kOe and 3.5 kOe, appears at $H_\perp = 4.0$ kOe. This drastic change is accounted for by the fact that the application of $H_\perp$ reduces the magnetic energy at the vertices. This reduction decreases the energy difference between $\langle +++\rangle$ or $\langle ---\rangle$ magnetic structures and $\langle ++-\rangle$ or $\langle +--\rangle$ magnetic structures. Here we define $H_{SW}$ as a field where the resistance charges abruptly. Figure 5(c) displays the perpendicular field $H_\perp$ dependence of $H_{SW}$. All of $H_{SW}$'s decrease, with increase in the perpendicular field $H_\perp$, because the latter reduces the in-plane component of the magnetization in the wire. With perpendicular fields of less than 3.60 kOe the number of the magnetization reversal is *two*, which shows that the ice-rule dominates the magnetization process in response to $H_\parallel$. For $H_\perp > 3.60$ kOe ($=H_{\perp C}$), clearly, a new jump labeled $H_{SW2}$ appears. Such a *three*-step magnetization reversal shows that the ice rule is lifted for $H_\perp > 3.60$ kOe.

The effective vertex energy $J$ can be roughly estimated from the magnetoresistance data in Fig. 5(c), since the ice-rule transition is argued in terms of competition between the Zeeman-energy and vertex-energy gains; $\Delta E \equiv E(\langle +++\rangle$ or $\langle ---\rangle, H_{SW2}) - E(\langle +--\rangle$ or $\langle ++-\rangle, H_{SW2}) = 0$ at $H_\perp = H_{\perp C}$ [Eq. (3)] and $\Delta E > 0$ for $H_\perp > H_{\perp C}$, where $E(\langle +++\rangle$ or $\langle ---\rangle, H_{SW2})$ is $E(\{\mathbf{M}_i\})$ for a $\langle +++\rangle$ or $\langle ---\rangle$ configuration at $H_{SW2}$. We calculated $\Delta E(\{\mathbf{M}_i\})$ for various $H_\perp$ values and estimated $J$ by comparing the calculation with the experiment. In the calculation, thermal fluctuation is neglected and $\mathbf{M}_i$ in Eq. (1), corresponding to the in-plane component of the magnetization of the $i$th wire, is assumed to decrease linearly with $H_\perp$;[19] the latter assumption is well justified by a magnetization measurement for single wire with a similar cross-sectional dimension (not shown here). To determine $4J|\mathbf{M}_i|^2$, i.e., the energy difference between the $\Sigma_{i \in N}\mathbf{M}_i \neq 0$ configuration and the $\Sigma_{i \in N}\mathbf{M}_i = 0$ configuration, from Eq. (3), we assumed the saturated magnetization $M_S = 1.08$ Wb/m$^2$, the effective in-plane magnetic moment in a wire $\mathbf{M}' = 2.4 \times 10^{-22}$ Wb·m, and the switching field $H_{SW2} = 0.21$ kOe at $H_\perp = 3.60$ kOe. The estimated $4J|\mathbf{M}_i|^2$ is $1.8 \times 10^{-17}$ J; this energy value is much larger than the thermal energy at room temperature, which indicates that the magnetic-ice order in this system is quite stable over a wide temperature range.

## VI. SUMMARY

We have investigated the remanent magnetic structures and the magnetization processes in a permalloy wire-based honeycomb network system by using MFM and magnetoresistance measurements. The MFM measurement shows that the magnetic configuration at each vertex is governed by vertex interaction similar to the ice rule, and an analogy between the present honeycomb structure and an Ising system on a kagomé lattice. The magnetoresistance measurement reveals that the magnetic-ice rule also dominates the magnetization process in the network. We found that the application of perpendicular magnetic field $H_\perp$ can suppress the magnetic ice rule, which results in a drastic change of the magnetization process of the network.

## ACKNOWLEDGMENT

*Electronic address: mtanaka@phys.keio.ac.jp

[1] U. Ruediger, J. Yu, S. Zhang, A. D. Kent, and S. S. P. Parkin, Phys. Rev. Lett. **80**, 5639 (1998).

[2] Y. Otani, S. G. Kim, K. Fukamichi, O. Kitakami, and Y. Shimada, IEEE Trans. Magn. **34**, 1096 (1998).

[3] J. E. Wegrowe, D. Kelly, A. Franck, S. E. Gilbert, and J. P. Ansermet, Phys. Rev. Lett. **82**, 3681 (1999).

[4] T. Taniyama, I. Nakatani, T. Namikawa, and Y. Yamazaki, Phys. Rev. Lett. **82**, 2780 (1999).

[5] S. Kasai, T. Niiyama, E. Saitoh, and H. Miyajima, Appl. Phys. Lett. **81**, 316 (2002).

[6] J. L. Tsai, S. F. Lee, Y. D. Yao, C. Yu, and S. H. Liou, J. Appl. Phys. **91**, 7983 (2002).

[7] L. Malkinski, R. E. Camley, Z. Celinski, T. A. Winningham, S. G. Whipple, and K. Douglas, J. Appl. Phys. **93**, 7325 (2003).

[8] D. A. Allwood, Gang Xiong, M. D. Cooke, C. C. Faulkner, D. Atkinson, N. Vernier, and R. P. Cowburn, Science **296**, 2003 (2002).

[9] E. Saitoh, M. Tanaka, H. Miyajima, and T. Yamaoka, J. Appl. Phys. **93**, 7444 (2003).

[10] F. J. Castaño, K. Nielsch, C. A. Ross, J. W. A. Robinson, and R. Krishnan, Appl. Phys. Lett. **85**, 2872 (2004).

[11] M. Tanaka, E. Saitoh, H. Miyajima, and T. Yamaoka, J. Magn. Magn. Mater. **282**, 22 (2004).

[12] Y. C. Chen, Y. D. Yao, S. F. Lee, Y. Liou, J. L. Tsai, and Y. A. Lin, Appl. Phys. Lett. **86**, 053111 (2005).

[13] M. Tanaka, E. Saitoh, H. Miyajima, T. Yamaoka, and Y. Iye, J. Appl. Phys. **97**, 10J710 (2005).

[14] E. Saitoh, K. Harii, H. Miyajima, T. Yamaoka, and S. Okuma, Phys. Rev. B **71**, 172406 (2005).

[15] A. P. Ramirez, A. Hayashi, R. J. Cava, R. Siddharthan, and B. S. Shastry, Nature **399**, 333 (1999).

[16] A. P. Ramirez, G. P. Espinosa, and A. S. Cooper, Phys. Rev. B **45**, 2505 (1991).

[17] M. J. Harris, S. T. Bramwell, D. F. McMorrow, T. Zeiske, and K. W. Godfrey, Phys. Rev. Lett. **79**, 2554 (1997).

[18] Z. Hiroi, K. Matsuhira, S. Takagi, T. Tayama, and T. Sakakibara, J. Phys. Soc. Jpn. **72**, 411 (2003).

[19] S. Chikazumi, *Physics of Ferromagnetism*, 2nd ed. (Oxford University Press, Oxford, 1997).